DOI: 10.1002/vms3.1079

ORIGINAL ARTICLE

WILEY

Radiologic features of radiolucent foreign bodies ingestion in common mynah (*Acridotheres tristis*)

Mohammad Molazem[1,2] | **Sarang Soroori**[1] | **Reihaneh Soflaei**[1] | **Alireza Bahonar**[3] | **Seyed Ahmad Madani**[4] | **Roshanak Mokhtari**[1] | **Antje Hartmann**[5]

[1]Faculty of Veterinary Medicine, Department of Veterinary Surgery and Diagnostic Imaging, University of Tehran, Tehran, Iran

[2]Faculty of Veterinary Medicine, Department of Radiology, University of Bern, Bern, Switzerland

[3]Faculty of Veterinary Medicine, Department of Food Hygiene and Quality, University of Tehran, Tehran, Iran

[4]Faculty of Veterinary Medicine, Department of Animal and Poultry Health and Nutrition, University of Tehran, Tehran, Iran

[5]Department for Diagnostic Imaging, Veterinary Clinic Hofheim, Hofheim am Taunus, Germany

Correspondence
Sarang Soroori and Reihaneh Soflaei, Faculty of Veterinary Medicine, Department of Veterinary Surgery and Diagnostic Imaging, University of Tehran. Dr. Gharib St., Azadi St., Tehran 1419963111, Iran.
Email: Soroori@ut.ac.ir; Reihanehsoflaie@yahoo.com

Abstract

Background: In mynahs with foreign body ingestion, delayed diagnosis increases the risk of poor outcomes.

Objective: The aim of this study was to evaluate various radiologic features on plain and contrast radiographs in mynahs for assessing the presence of ingested foreign bodies.

Methods: In our cross-sectional study, a total of 41 mynahs were included. The diagnosis was made by history, surgery, excision by forceps or excretion in the faeces. Overall, 21 mynahs were considered not to have a foreign body in their gastrointestinal tract. Plain and post-contrast [oral administration of barium sulphate colloidal suspension of 25% weight/volume (20 mg/kg)] lateral and ventrodorsal radiographs from the cervical and coelomic cavity were taken. Different parameters including oesophageal, proventricular, and small intestinal diameters and opacities were assessed. Image evaluation was performed by two national board-certified radiologists blinded to the final diagnoses.

Results: The inter- and intra-observer reliabilities of the diagnostic features were significant ($p < 0.001$). The diagnosis of the foreign body was highly accurate [90.2% (95% CI: 76.9%, 92.3%)] with the sensitivity, specificity, and area under the representative characteristic curve of 90.0%, 90.5%, and 0.93%, respectively for plain radiographs. The size and opacity of the oesophagus, proventriculus, and intestinal loops as well as serosal details were significantly different between mynahs with and without foreign body intake ($p < 0.05$).

Conclusions: Lateral and ventrodorsal plain radiographs are highly reliable for diagnosing the presence of non-opaque obstructing objects in the gastrointestinal tract of mynahs. Attention should be paid to the size and opacity of the oesophagus, extension, and opacity of the proventriculus, segmental opacity of intestinal loops, and decrease in serosal details.

KEYWORDS
coelomic cavity, gastrointestinal obstruction, imaging, mynah, non-opaque obstructing object, radiography

1 | INTRODUCTION

Common mynah (*Acridotheres tristis*) is an opportunist omnivorous bird native to Asia (Kadhim et al., 2013) but is now found throughout the world (Ishtiaq et al., 2006). Although mynah is considered a pet bird in Asia, it is not a domestic animal. It has been adapted to locate food on the ground in grassland and short lawns as the favoured feeding areas (Feare et al., 2017). The bird is attracted to insects, human food waste, or ripened fruits on trees (Zuccon et al., 2006). The neutral mucin of the lingual salivary glands in the mynah serves as a lubricant to facilitate swallowing (Kadhim et al., 2013). Some ingested objects can expand in the gastrointestinal tract (Miller et al., 2009).

Ingestion of foreign bodies (FBs) is common in avian patients (Adamcak et al., 2000; Cannon, 2006; Wagner, 2005). Affected birds are presented with anorexia, weight loss, and dark malodorous stool. Physical examinations may reveal a palpable mass in the crop of the bird, and laboratory tests show anaemia (Adamcak et al., 2000; Wells, 1984). Mynahs does not have a crop. Some patients with gastrointestinal FBs are diagnosed late because the signs are nonspecific (Wagner, 2005). Delayed diagnosis, in turn, increases the risk of poor outcomes. Imaging plays an important role in the initial diagnosis of ingested FBs, localisation, recognition of complications, and guiding the clinical management of the condition (Adamcak et al., 2000).

While the intake of metallic FBs has been described frequently, there is a relative paucity of information regarding the ingestion of radiolucent substances in birds (Wagner, 2005). Commonly, radiographs show gas-filled dilated proventriculus and intestinal loops (Adamcak et al., 2000). The filling defect in the barium contrast study suggests the presence of a radiolucent object (Adamcak et al., 2000). Ultrasonography provides complementary diagnostic information for gastrointestinal tract problems in birds (Elser et al., 2020; Krautwald-Junghanns et al., 2002; Wagner, 2005). However, for a high-quality sonographic image, the gastrointestinal tract should be emptied of gas and ingesta which is not usual in avian imaging (Krautwald-Junghanns et al., 2002).

The diagnostic accuracy of radiography of the gastrointestinal tract depends on a variety of conditions (Elser et al., 2020). Abdominal radiographs are taken in dogs and cats with clinical signs of gastrointestinal obstruction. Segmental dilation of the small intestine, plication, bunching, and abnormal luminal gas opacities are common radiological signs of mechanical obstruction in small animals (Elser et al., 2020; Lamb & Hansson, 1994; Wagner, 2005). However, the accuracy of subjective assessment of radiographs to diagnose gastrointestinal mechanical obstruction ranges from 61% to 89.1% in cats and dogs (Elser et al., 2020; Sharma et al., 2011; Zatloukal et al., 2004).

The present study aims to assess the value of different subjective and objective imaging features for diagnosing non-radiopaque FBs ingested in mynahs. We hypothesised that mynahs with alimentary FBs would show an increase in the diameters of the proventriculus and the small intestines and that mynahs with alimentary FBs, depending on the location and size, would show an increase in the diameters of the GI tract.

2 | MATERIALS AND METHODS

2.1 | Design and setting

This research is a descriptive cross-sectional study to assess different radiographic imaging features and objective parameters for diagnosing radiolucent FBs. It was conducted prospectively from April 2018 to January 2021 in the Department of Imaging at a Small Animal Hospital. The hospital is a referral centre affiliated with the faculty of Veterinary of a University. The study was carried out in accordance with the Guidelines for the Care and Use of Experimental Animals. Ethics approval was obtained from the Institutional Review Boards of the University.

2.2 | Patients

We included mynahs brought in by their owners with suspicion of ingestion of a FB. Any history of current illness, decreased food intake, vomiting, diarrhoea and obstipation was recorded. All patients were examined for a palpable mass and then, radiography was carried out under physical restriction. Mynahs showing a radiopaque FB on radiographs were excluded from the study. Based on the clinical history provided by the owner, as well as clinical and radiological findings Mynahs were divided into two groups: 20 mynahs suffering from an alimentary FB and 21 mynahs not suffering from an alimentary FB. The final diagnosis was made by history, surgery, excision by forceps or excretion in the faeces.

2.3 | Radiography

A resident of radiology carried out all radiographic steps under the supervision of a board-certified radiologist. Initial lateral and ventrodorsal radiographs were taken from the neck and coelomic cavity. Then, post-contrast radiography was performed with barium sulphate colloidal suspension of 25% weight/volume (20 mg/kg), administered orally with a syringe. Next, radiographs were taken at baseline, 30 min, and 1–3 h later. All radiographs were taken with the same x-ray unit (Kodak Carestream Directview Classic CR, Toshiba, Minato, Japan)

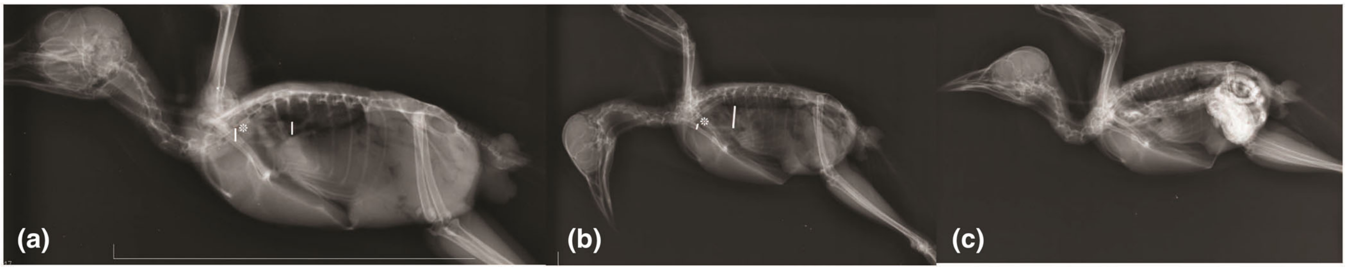

FIGURE 1 Comparison of the thoracic inlet tracheal diameter with maximum oesophageal diameter in lateral projections. (a) Plain lateral view in a normal common mynah shows no sign of oesophageal dilation with a ratio of 0.83 (score number of 0). (b, c) Plain and post-contrast lateral radiographs (obtained 5 min after administration of barium sulphate colloidal suspension 25% weight/volume (20 mg/kg) show severe dilation of the coelomic oesophagus, proventricle and gizzard. In (b), oesophagus to tracheal diameter ratio is 3.75 (score number of 2). In (c), the linear FB (hair band) has been delineated from the coelomic oesophagus up to the gizzard.

with a focal-film distance of 75 cm, and an exposure of 40 kV and 8 mAs. Images were recorded in a Picture Archiving and Communication System. Patients' data were anonymised and an arbitrary number was assigned to each bird.

2.4 | Outcome measures

Two national board-certified radiologists (radiologists A and B), blinded to patients' history and physical examination, read all plain and post-contrast radiographic images in two phases with a one-month interval and in a random sequence. The diameter and opacity of the oesophagus, the proventriculus, and the small intestines, as well as the serosal details, were assessed. The diameter was measured on plain and post-contrast radiographs. The opacity was only assessed on plain radiographs. The oesophageal diameter was assessed on lateral radiographs in comparison with the tracheal diameter at the level of thoracic inlet: Grade 0 was given if the oesophageal diameter was equal to the tracheal height, grade 1 was given if it was less than twice the tracheal height and grade 2 was given if it was equal or more than twice the tracheal height (Figure 1).

To determine the size of the proventriculus, multiple measurements have been performed. On the lateral radiograph, an index line from the most caudoproximal point of the articulation of the coracoid with the scapula was drawn until the cranioventral border of pygostyle and the extension of the proventriculus dorsal to this index line was recorded (Figure 2, a and c). The recording was done subjectively by grading the extension dorsal to this line as none (0), mild (1), moderate (2) or severe (3). In addition, absolute measurements were performed by measuring the length of proventricular extension above the reference line. On ventrodorsal radiographs, two values were assessed. First, a ratio of cardiac width to the maximum liver plus proventriculus silhouette (caudal part of the 'hourglass shadow') was calculated. Second, a ratio between the right and left extension of the caudal part of the 'hour class shadow' from the midline (vertebrae sternum silhouette) was calculated (right-to-left ratio in caudal hourglass shadow) (Figure 2, b and e).

Assessment of opacity of the oesophagus and proventriculus was done subjectively (gas opaque = 0, soft tissue = 1, bone opaque = 2, mineral opaque = 3) as well as in comparison to the opacity of the last thoracic vertebra and pectoralis muscle, with a value of −1 given if the opacity was below the respective reference structure, 0 if it was equal and 1 if it was greater.

Three different values were calculated to assess the intestinal loop diameter (ILD). First, a ratio of ILD to the distal femoral diaphysis diameter (DFD) at the level of the proximal border of the patella was calculated (ILD/DFD). Second, a ratio between ILD and the last thoracic vertebral body length (TVL) was calculated (ILD/TVL) (Figure 3). In addition, a subjective assessment of the percentage of gas-dilated bowel loops [segmental (less than 25%), regional (25%–50%), and diffuse (more than 50%)] was performed. We also recorded subjective judgment for the presence of gastrointestinal FB (not present = 0, present = 1, and not sure = 2) and serosal details (normal = 0, decreased less than 50% = 1, decreased more than or equal to 50 % = 2, and presence of free coelomic gas = 3).

2.5 | Statistical analyses and sample size

Results are presented as mean (SD) for continuous variables, and as absolute numbers (%) for categorical data. The means of the continuous variables were compared using independent samples *t*-tests. Either a χ^2 or Fisher's exact test was used in testing differences among the study groups for categorical variables. We used Cohen's kappa coefficient for evaluating the reliability of categorical diagnostic features and the intra-class correlation coefficient for interval variables. The results are presented as the coefficient with a 95% confidence interval and a *p* value. The diagnostic value of models is described as accuracy with a 95% confidence interval, sensitivity, specificity and the area under the representative characteristic curve (ROC). The level of significance was set at two-tailed $\alpha = 0.05$. Overall, we needed 34 mynahs to estimate the 95% confidence interval of the area under ROC with the ratio of not ingested to ingested FB of 1, a false-positive rate of 10%, a true positive rate of 80%, and a width of 20% for estimating the confidence

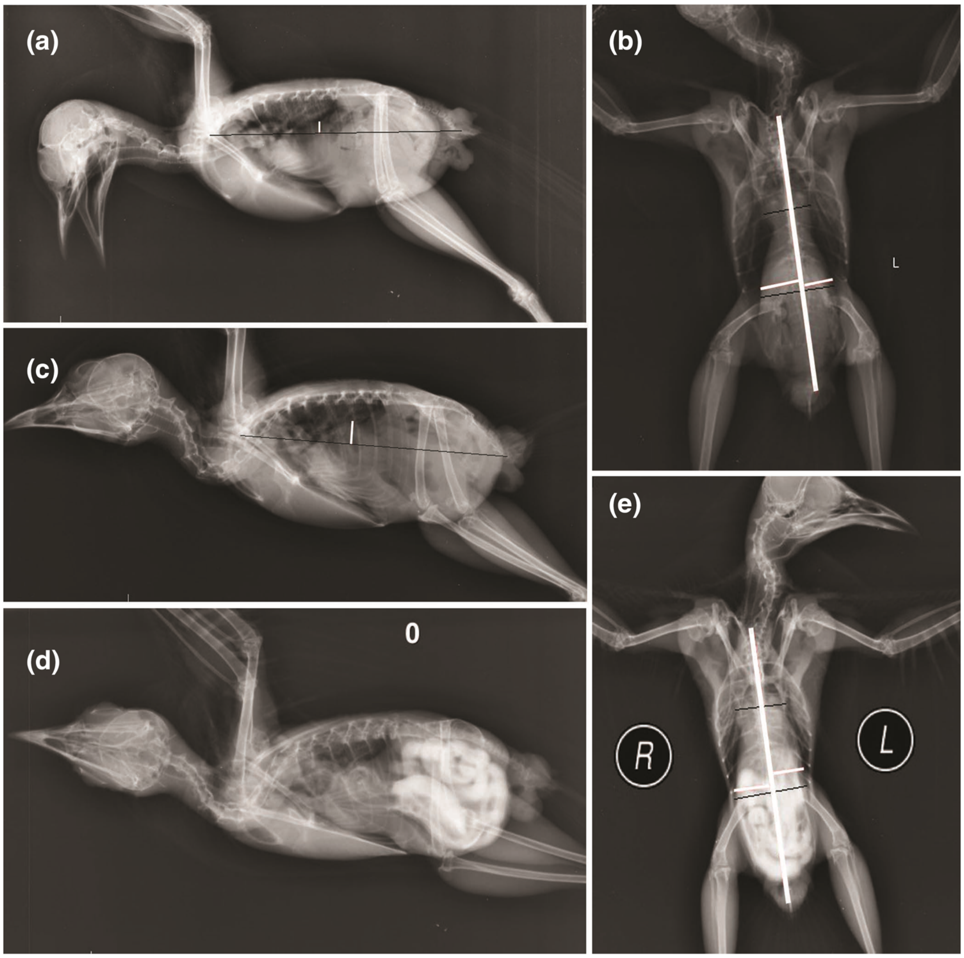

FIGURE 2 Proventricular evaluations: (a, b) Plain Lal and VD views in a normal Common Mynah. In (a) an index line (black line) is drawn from the most caudoproximal point of the coracoid bones until the cranoventral border of pygostyle and the degree of proventricular dilation, extending above the index line is determined (3.5 mm). In (b) the maximum cardiac breadth is measured and compared with the maximum liver plus proventriculus silhouette (the caudal hourglass portion), in addition, a straight line is drawn on the vertebraesternum silhouette, and the width of the right and left most dilated aspect of the caudal hourglass is also measured. (c–e) Plain Lat and post contract Lat and VD projections from a Mynah that is swallowed a hair band. (c) The extension from the index line is 10 mm. (d) Hairband has been located in the proventricle and gizzard. In (e), the caudal hourglass appearance has been disturbed.

FIGURE 3 Intestinal evaluations (normal): the maximum intestinal loop dilation is evaluated by comparing with distal femoral diaphysis diameter at the level of the patella and the maximum vertebral body length of the last thoracic vertebra.

TABLE 1 Reliability of radiologic features of oesophagus assessed by radiologists A and B. For categorical features, the results represent the kappa coefficient with a 95% confidence interval and for interval features the results represent the intra-class correlation coefficient with a 95% confidence interval (All $p < 0.001$)

Imaging	Feature			Inter-observer *(95% CI)	Intra-observer* (95% CI)	
				A vs. B	A	B
Plain	Size			0.93 (0.88, 0.96)	0.79 (0.63, 0.88)	0.98 (0.96, 0.99)
	Opacity	Normalised with thoracic vertebrae	Cervical	0.88 (0.65, 1)	1 (1, 1)	0.88 (0.65, 1)
			Coelomic	0.93 (0.81, 1)	1 (1, 1)	1 (1, 1)
		Normalised with pectoralis muscle	Cervical	0.88 (0.65, 1)	1 (1, 1)	0.88 (0.65, 1)
			Coelomic	0.86 (0.68, 1)	1 (1, 1)	1 (1, 1)
		Subjective		0.93 (0.79, 1)	1 (1, 1)	1 (1, 1)
Contrast	Size			0.96 (0.92, 0.98)	0.94 (0.88, 0.97)	0.93 (0.88, 0.96)

*All $p < 0.001$.

interval. We added 5 more patients to maintain test powers, totalling 41 mynahs. All data analyses were performed with R version 3.5.0 for windows. R is a well-known open-source environment for computing and graphics (https://www.r-project.org/).

3 | RESULTS

3.1 | Sample

In total, radiographs from 41 mynahs were included in our study; 20 mynahs were considered of suffering from a radiolucent alimentary FB based on clinical history and examination, and 21 mynahs were considered not to have an alimentary FB. Of the 20 cases of ingested FBs, 8 were in the gizzard; 7 were in the proventriculus and gizzard; 1 in the gizzard and intestine; 1 in the coelomic oesophagus, proventricle and gizzard; 1 in the oropharynx cavity, oesophagus, proventricle and gizzard; 1 in the cranial coelomic oesophagus, proventricle and gizzard; and 1 in caudal cervical and coelomic oesophagus, proventricle, gizzard and intestine. In general, the FBs included hair bands, ribbons, elastic bands, yarns and strings.

3.2 | Reliability and comparisons

Table 1 shows the reliability of the measurements on the oesophagus. All inter- and intra-observer reliabilities were significant and large; therefore, we compared the measurements carried out by one of the radiologists (radiologist A). Plain radiography showed that the diameter of the oesophagus was larger in mynahs with FB ingestion (MFBI) [1.28 (0.87) vs. 0.86 (0.17) mm, *t*-test $p = 0.043$].

The opacity of the cervical oesophagus did not show significant differences between the two groups. However, the opacity of the coelomic oesophagus normalised with thoracic vertebra or pectoralis muscle was significantly different between MFBI compared to those without FBI on plain radiography (both χ^2 test $p = 0.010$). The opacity of the coelomic oesophagus normalised with the thoracic vertebra was commonly rated as 0 (11/20) and 1 (7/20) in MFBI, and 0 (20/21) in the normal group. For the coelomic opacity normalised with pectoralis muscle, 0 (11/20) and 1 (8/20) were common in MFBI, and 0 (20/21) was the most frequently observed opacity in the normal group.

Table 2 illustrates the reliability of the measurements on the proventriculus. Overall, the inter- and intra-observer reliabilities were significant and large, except for the right-to-left ratio caudal hourglass shadow which was not significant. On plain radiography, the difference in subjective assessment of the dorsal extension of the proventriculus was significant (χ^2 test $p = 0.001$). The dorsal extension was most commonly rated as 3 (11/20) and 2 (10/21) in MFBI and normal groups, respectively. The difference in the value of dorsal extension from the index line [5.74 (2.77) vs. 3.74 (1.32) mm, *t*-test $p = 0.007$] was also significant and the optimal cut-point was 6.1 mm with the accuracy, sensitivity, specificity, and area under ROC of 78%, 55%, 100%, and 0.71, respectively. The opacity of the proventriculus normalised with the thoracic vertebra was significantly different (χ^2 test $p < 0.001$). In the MFBI group opacity was grade 1 (11/20) and in the healthy group, it was grade 0 (20/21). For the opacity of proventriculus normalised with pectoralis muscle, the result was also significant (χ^2 test $p < 0.001$) with a higher frequency of grade 1 (12/20) in the MFBI group and grade 0 (20/21) in the healthy group.

Table 3 shows the reliability of the measurements on intestinal loops. Large and significant inter- and intra-observer reliabilities indicate that the radiologic features are highly reliable in the diagnosis of radiolucent FBs. The percentage of gas-dilated bowel loops was diffuse with more than 50% of gas-dilated small intestinal loops in 50% of the birds (10/20); while for healthy mynahs, segmental opacity (17/21) was more prevalent (χ^2 test $p < 0.001$). Serosal details commonly were categorised as 'decreased less than 50%' (9/20) and 'decreased more than or equal to 50 %' (9/20) in MFBI; however, in healthy birds, the serosal details (18/21) were unchanged (χ^2 test $p < 0.001$). In post-contrast radiography, the opacity of intestinal loops was similar to plain radiography (χ^2 test $p < 0.001$). Other comparisons were not significant (all $p > 0.05$)

TABLE 2 Reliability of radiologic features of proventriculus assessed by radiologists A and B. For categorical features, the results represent the kappa coefficient with a 95% confidence interval and for interval features, the results represent the intra-class correlation coefficient with a 95% confidence interval

Imaging	Measure	Feature	Inter-observer* (95% CI)	Intra-observer* (95% CI)	
			A vs. B	A	B
Plain	Size	CPL	0.92 (0.85, 0.96)	0.59 (0.35, 0.76)	0.56 (0.31, 0.74)
		Right-to-left ratio of caudal hourglass shadow	0.6 (0.36, 0.77)	0.27 (−0.04, 0.53)	0.16 (−0.16, 0.44)
		Subjective assessment of dorsal extension	0.44 (0.25, 0.63)	0.59 (0.41, 0.78)	0.83 (0.69, 0.97)
		Dorsal extension of the proventriculus	0.9 (0.82, 0.95)	0.9 (0.83, 0.95)	0.99 (0.99, 1)
	Opacity	Normalised with thoracic vertebra	0.89 (0.73, 1)	0.94 (0.84, 1)	0.94 (0.82, 1)
		Normalised with pectoralis muscle	0.94 (0.83, 1)	0.94 (0.83, 1)	1 (1, 1)
		Subjective	1 (1, 1)	1 (1, 1)	1 (1, 1)
Contrast	Size	CPL	0.9 (0.74, 0.95)	0.82 (0.68, 0.9)	−0.02 (−0.33, 0.29)
		Right-to-left ratio of caudal hourglass shadow	0.64 (0.41, 0.79)	0.69 (0.5, 0.82)	0.93 (0.81, 1)
		Subjective assessment of dorsal extension	0.5 (0.3, 0.69)	0.49 (0.29, 0.69)	0.69 (0.51, 0.87)
		Extension from the index line	0.79 (0.63, 0.89)	0.83 (0.7, 0.91)	0.95 (0.91, 0.97)

**p* Value for intra-rater reliability of Caudal hourglass on plain radiography were 0.045 and 0.165 for radiologists A and B, respectively. For radiologist B, the *p* value of intra-rater reliability of CPL in post-contrast radiography was 0.557. All other $p < 0.001$.
CPL: cardiac width/(proventriculus width+ liver width).

TABLE 3 Reliability of radiologic features of intestinal loops assessed by radiologists A and B. For categorical features, the results represent the kappa coefficient with a 95% confidence interval and for interval features, the results represent the intra-class correlation coefficient with a 95% confidence interval

Imaging	Feature		Inter-observer(95% CI)*	Intra-observer (95% CI)*	
			A vs. B	A	B
Plain	Size	ILD/FDD	0.87 (0.76, 0.93)	0.49 (0.22, 0.69)	0.45 (0.17, 0.66)
		ILD/VBL	0.78 (0.63, 0.88)	0.54 (0.28, 0.72)	0.46 (0.18, 0.67)
	Opacity		0.88 (0.75, 1)	1 (1, 1)	0.88 (0.75, 1)
	Subjective diagnosis of radiolucent FB		1 (1, 1)	1 (1, 1)	0.91 (0.79, 1)
	Serosal details		0.96 (0.89, 1)	0.96 (0.89, 1)	0.96 (0.89, 1)
Contrast	Size	ILD/FDD	0.80 (0.65, 0.89)	0.75 (0.57, 0.86)	0.80 (0.65, 0.89)
		ILD/VBL	0.95 (0.89, 0.98)	0.96 (0.93, 0.98)	0.78 (0.63, 0.88)
	Opacity		0.96 (0.88, 1)	1 (1, 1)	0.88 (0.75, 1)
	Subjective diagnosis of radiolucent FB		1 (1, 1)	1 (1, 1)	1 (1, 1)

*All $p < 0.001$.
ILD: intestinal loop diameter, FDD: femoral diaphysis diameter, VBL: vertebral body length, FB: foreign body.

3.3 | Diagnostic accuracy

Both radiologists' diagnosis of radiolucent FBs showed accuracy (95% CI), sensitivity, and specificity of 90.2% (76.9%, 92.3%), 90.0% and 90.5% for the first try with a similar area (0.93) under the ROC (Figure 4). On the second try, the results remained the same for radiologist A. However, for radiologist B, accuracy, sensitivity, and specificity decreased to 85.3% (70.8%, 94.4%), 80.0%, and 90.5% and the area under the ROC changed to 0.92. This showed that the 1-month interval between two readings of radiographs had decreased the potential for recalling the cases.

4 | DISCUSSION

We conducted this study to evaluate the reliability and diagnostic accuracy of various imaging features on plain and contrast radiography of mynahs suspected of ingesting non-opaque FBs. Our study showed that some of the radiographic measurements would help the radiologist to detect radiolucent FBs. We found that inter- and intra-observer reliabilities of the diagnostic features were significant and large and that the anatomical changes following intake of FBs would help to diagnose obstruction in the absence of a discernable opaque object.

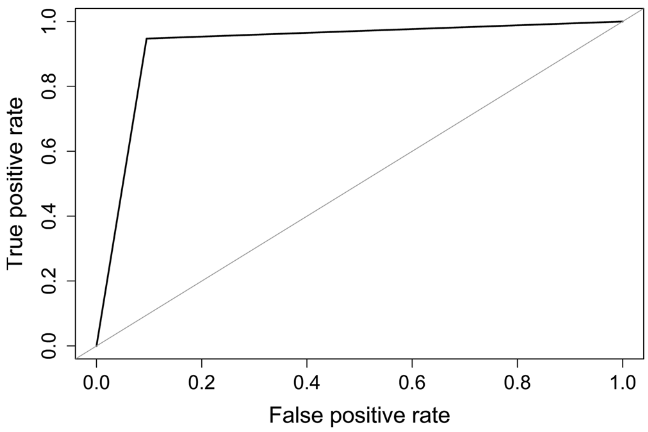

FIGURE 4 The ROC for both radiologists' diagnosis of radiolucent FBs on the first try (Area under the curve = 0.93).

On plain radiography, the size of the coelomic oesophagus was larger if a FB had been ingested. In some animals this can be due to the fact that the FB itself was located within the coelomic part of the oesophagus, however, dilation was present also in birds in which the FB was not located within the oesophagus. This might be because the presence of a FB within the proventriculus and/or gizzard might prevent food to enter the stomach, leading to the accumulation of food in the coelomic oesophagus which shows the reflux of gastric contents into the coelomic oesophagus. Lack of dilation of the cervical oesophagus can either be due to the fact that food or gastric contents do not back up to the level of the cervical portion. However, it can also be because the cervical oesophagus lies embedded in other soft tissue structures preventing clear delineation of its walls in comparison to the coelomic oesophagus which lies surrounded by gas-filled structures making identification easier. Thus, false negative results for the cervical oesophagus cannot fully be excluded, however, they are considered a less likely explanation as the neck of the mynah is thin and relevant dilation of the cervical oesophagus would presumably lead to a visible increase in diameter of the neck.

The opacity of the coelomic oesophagus, normalised with the thoracic vertebra or pectoralis muscle, was higher in MFBI. These facts might support the above-mentioned theory of food backing up in the coelomic part of the oesophagus, not being able to enter the stomach, and leading to dilation and increased opacity of this part of the oesophagus.

In patients with FB ingestion, the proventriculus seemed more extended and the extension was farther from the index line with the cut-point of 6.1 mm. Our study suggested that more than 5 mm extension from the index line is indicative of the presence of FB in the proventriculus for the cases that are suspected of FB ingestion. The opacity of the proventriculus normalised with the thoracic vertebra or pectoralis muscle was greater in MFBI than in normal mynahs.

Only half of the MFBI show diffuse gas distributions in bowel loops. This may explain the difference in the time it takes to swallow a FB until radiographs are taken, or the difference in the size of the FB causing an obstruction. The opacity of intestinal loops was commonly segmental in healthy mynahs.

A loss of serosal details was seen in about half of MFBI, whereas only three Mynahs without FB ingestion have a reduction in serosal details. In none of the patients with decreased serosal details, contrast leakage from the gastrointestinal tract has been detected, which shows partial obstruction did not lead to perforation and peritonitis in our study. It can be secondary due to infiltration as a subsequence of partial obstruction. It can also be due to the reduction of coelomic cavity fat deposition if the animals are already suffering from the FB for a longer time leading to decreased food intake. Further studies are needed on possible perforation and peritonitis in larger Mynahs populations.

Most of the FBs were found in the gizzard followed by the proventriculus. The FBs dilated the gizzard and consequently, displaced the intestines caudoventrally and caudodorsally. The dilated gizzard was more commonly inclined to the right. The size of the caudal hourglass was not changed observably and its right-to-left ratio was fixed, as well. With the FB in the proventriculus, the middle hourglass had a rather distorted shape, particularly on the left side. In MFBI, the contrast substance reached the cloaca in more than 90 min. This time was less than 45 min in normal cases. This could be attributed to gastrointestinal hypomobility following obstruction.

Our study showed that diagnosing radiolucent FBs with radiographic landmarks on plain radiographs could be accurate, sensitive, and specific. Considering the high intra and inter-observer reliabilities of the measurements and the large area under the ROC, plain lateral and ventrodorsal radiographs in accompaniment with post-contrast radiography are recommended for diagnosing radiolucent FBs in mynahs. Our studied landmarks were accurate, sensitive, and specific on plain radiographs. Meanwhile, the usage of diagnostic features on plain radiographs requires a larger sample size. Until providing stronger evidence, contrast radiography is still needed for diagnosing non-opaque FBs. Overall, our results are in accordance with the results of some previous studies carried out on other animals.

Diagnosis of gastrointestinal obstruction with radiographs requires the observer's experience and parameters for the assessment of anatomical structures (Garrett et al., 2019; Graham et al., 1998; Kleine & Lamb, 2005; Lamb & Hansson, 1994). Radiographic evaluations in 11 dogs and 5 cats showed that gastric or small intestinal distension and reduced serosal details are common in small animals with gastrointestinal FBs (Tyrrell & Beck, 2006). In a survey of abdominal radiographs from dogs, a ratio of the maximum small intestinal diameter and the height of the body of the fifth lumbar vertebra at its narrowest point was used successfully for the diagnosis of intestinal obstruction (Graham et al., 1998).

Our study confirmed that in mechanical obstructions, the size of the anatomical silhouette would be a reliable clue to the presence of an obstructing object. Our results suggested that oesophagus or intestine size or any displacement and extension were significantly different between MFBI and healthy mynahs. Although, intestinal dilation is not pathognomonic of FB obstruction (Graham et al., 1998). Fluid and gas retention proximal to the site of obstruction is the reason for distension, particularly if FB lodges distal in the gastrointestinal tract (Papazoglou et al., 2003). Also, inflammation and alteration to the intestinal layering at the site of obstruction and a decrease in intra-abdominal fat lead to loss of intestinal layering and reduced serosal details (Tyrrell & Beck, 2006).

5 | CONCLUSION

To our knowledge, this is the first report describing radiographic features of non-radiopaque FB in mynahs and their diagnostic accuracy and reliability. Dilation of the coelomic oesophagus, increased opacity normalised to either thoracic vertebra or pectoralis muscle, an extension of the proventriculus of more than 5 mm above a line from most caudoproximal point of the articulation of the coracoid with the scapula to the cranioventral border of pygostyle are highly reliable radiographic signs on plain radiography for diagnosing the presence of non-opaque obstructing objects with high sensitivity and specificity. In addition, a decrease in serosal details on plain radiographs should raise suspicion of the presence of a FB.

AUTHOR CONTRIBUTIONS

Mohammad Molazem: conceptualization; formal analysis; methodology; project administration; writing – original draft; writing – review & editing. Sarang Soroori: formal analysis; methodology; supervision; writing – original draft; writing – review & editing. Reihaneh Soflaei: conceptualization; data curation; investigation; resources; writing – original draft; writing – review & editing.

ACKNOWLEDGEMENT

None.

COMPETING INTERESTS

The authors declare that they have no competing interests.

FUNDING

This research did not receive any specific grant from funding agencies in the public, commercial or not-for-profit sectors.

DATA AVAILABILITY STATEMENT

The data that support the findings of this study are available from the corresponding author upon reasonable request.

ETHICS STATEMENT

Ethics approval was obtained from the Institutional Review Boards of the Faculty of Veterinary, University of Tehran, with the ethics code of: IR28200/6/16.

ORCID

Sarang Soroori https://orcid.org/0000-0002-0975-6731
Reihaneh Soflaei https://orcid.org/0000-0003-0733-4022

PEER REVIEW

The peer review history for this article is available at https://publons.com/publon/10.1002/vms3.1079.

REFERENCES

Adamcak, A., Hess, L. R., & Quesenberry, K. E. (2000). Intestinal string foreign body in an adult umbrella cockatoo (*Cacatua alba*). *Journal of Avian Medicine and Surgery*, *14*(4), 257–263.

Cannon, M. J. (2006). Unusual tracheal foreign body in an African grey parrot. *Veterinary Clinics of North America: Exotic Animal Practice*, *9*(3), 551–556. https://doi.org/10.1016/j.cvex.2006.05.005

Elser, E. B., Mai, W., Reetz, J. A., Thawley, V., Bagshaw, H., & Suran, J. N. (2020). Serial abdominal radiographs do not significantly increase accuracy of diagnosis of gastrointestinal mechanical obstruction due to occult foreign bodies in dogs and cats. *Veterinary Radiology & Ultrasound*, *61*(4), 399–408. https://doi.org/10.1111/vru.12870

Feare, C. J., van der Woude, J., Greenwell, P., Edwards, H. A., Taylor, J. A., Larose, C. S., Ahlen, P. A., West, J., Chadwick, W., Pandey, S., Raines, K., Garcia, F., Komdeur, J., & de Groene, A. (2017). Eradication of common mynas *Acridotheres tristis* from Denis Island, Seychelles. *Pest Management Science*, *73*(2), 295–304. https://doi.org/10.1002/ps.4263

Garrett, K., Milne, M., Doneley, R., & Perkins, N. (2019). Ultrasound evaluation of small intestinal thickness and a comparison to body weight in normal chickens (Gallus gallus domesticus). *Australian Veterinary Journal*, *97*(1–2), 39–42. https://doi.org/10.1111/avj.12777

Graham, J. P., Lord, P. F., & Harrison, J. M. (1998). Quantitative estimation of intestinal dilation as a predictor of obstruction in the dog. *Journal of Small Animal Practice*, *39*(11), 521–524. https://doi.org/10.1111/j.1748-5827.1998.tb03698.x

Ishtiaq, F., Beadell, J. S., Baker, A. J., Rahmani, A. R., Jhala, Y. V., & Fleischer, R. C. (2006). Prevalence and evolutionary relationships of haematozoan parasites in native versus introduced populations of common myna *Acridotheres tristis*. *Proceedings: Biological Sciences*, *273*(1586), 587–594. https://doi.org/10.1098/rspb.2005.3313

Kadhim, K. K., Hameed, A. T., & Abass, T. A. (2013). Histomorphological and histochemical observations of the common myna (*Acridotheres tristis*) tongue. *ISRN Veterinary Science*, *2013*, 980465. https://doi.org/10.1155/2013/980465

Kleine, L., & Lamb, C. (2005). Comparative organ imaging: The gastrointestinal tract. *Veterinary Radiology*, *30*, 133–141. https://doi.org/10.1111/j.1740-8261.1989.tb00762.x

Krautwald-Junghanns, M. E., Stahl, A., Pees, M., Enders, F., & Bartels, T. (2002). Sonographic investigations of the gastrointestinal tract of granivorous birds. *Veterinary Radiology & Ultrasound*, *43*(6), 576–582. https://doi.org/10.1111/j.1740-8261.2002.tb01052.x

Lamb, C. R., & Hansson, K. (1994). Radiological identification of nonopaque intestinal foreign bodies. *Veterinary Radiology and Ultrasound*, *35*(2), 87–88.

Miller, C. L., Bischoff, K. L., & Hoff, B. (2009). Polyacrylamide gel ingestion leading to fatal intestinal obstruction in two birds in a zoological collection. *Journal of Avian Medicine and Surgery*, *23*(4), 286–289. https://doi.org/10.1647/1082-6742-23.4.286

Papazoglou, L., Patsikas, M., & Rallis, T. (2003). Intestinal foreign bodies in dogs and cats. *Compendium on Continuing Education for the Practising Veterinarian – North American Edition*, *25*, 830-+.

Sharma, A., Thompson, M. S., Scrivani, P. V., Dykes, N. L., Yeager, A. E., Freer, S. R., & Erb, H. N. (2011). Comparison of radiography and ultrasonography for diagnosing small-intestinal mechanical obstruction in vomiting dogs. *Veterinary Radiology & Ultrasound*, *52*(3), 248–255. https://doi.org/10.1111/j.1740-8261.2010.01791.x

Tyrrell, D., & Beck, C. (2006). Survey of the use of radiography vs. ultrasonography in the investigation of gastrointestinal foreign bodies in small animals. *Veterinary Radiology & Ultrasound*, *47*(4), 404–408. https://doi.org/10.1111/j.1740-8261.2006.00160.x

Wagner, W. M. (2005). Small intestinal foreign body in an adult Eclectus parrot (*Eclectus roratus*). *Journal of the South African Veterinary Association*, *76*(1), 46–48. https://doi.org/10.4102/jsava.v76i1.395

Wells, S. (1984). Alimentary foreign body in an Amazon parrot. *Modern Veterinary Practice*, *65*(5), 385–386.

Zatloukal, J., Crha, M., Lorenzová, J., Husník, R., Kohout, P., & NeâAs, A. (2004). The comparative advantage of plain radiography in diagnosis of obstruction of the small intestine in dogs. *Acta Veterinaria Brno*, *73*(3), 365–374. https://doi.org/10.2754/avb200473030365

Zuccon, D., Cibois, A., Pasquet, E., & Ericson, P. G. (2006). Nuclear and mitochondrial sequence data reveal the major lineages of starlings, mynas and related taxa. *Molecular Phylogenetics and Evolution*, *41*(2), 333–344. https://doi.org/10.1016/j.ympev.2006.05.007

How to cite this article: Molazem, M., Soroori, S., Soflaei, R., Bahonar, A., Madani, S. A., Mokhtari, R., & Hartmann, A. (2023). Radiologic Features of Radiolucent Foreign Bodies Ingestion in Common Mynah (*Acridotheres tristis*). *Veterinary Medicine and Science*, 1–9. https://doi.org/10.1002/vms3.1079